DEVELOPMENTAL DYNAMICS 239:2404–2412, 2010

Characterization of the AP-1 μ1A and μ1B Adaptins in Zebrafish (*Danio rerio*)

Daniela Zizioli,[1] Elena Forlanelli,[1] Michela Guarienti,[1] Stefania Nicoli,[3] Alessandro Fanzani,[1] Roberto Bresciani,[1] Giuseppe Borsani,[1] Augusto Preti,[1] Franco Cotelli,[2]* and Peter Schu[4]*

Protein transport between the trans-Golgi network and endosomes is mediated by transport vesicles formed by the adaptor-protein complex AP-1, consisting of the adaptins γ1, β1, μ1, σ1. Mammalia express μ1A ubiquitously and isoform μ1B in polarized epithelia. Mouse γ1 or μ1A 'knock out's revealed that AP-1 is indispensable for embryonic development. We isolated μ1A and μ1B from *Danio rerio*. Analysis of μ1A and μ1B expression revealed tissue-specific expression for either one during embryogenesis and in adult tissues in contrast to their expression in mammalia. μ1B transcript was detected in organs of endodermal derivation and "knock-down" experiments gave rise to embryos defective in formation of intestine, liver, and pronephric ducts. Development ceased at 7–8 dpf. μ1B is not expressed in murine liver, indicating loss of μ1B expression and establishment of alternative sorting mechanisms during mammalian development. *Developmental Dynamics 239:2404–2412, 2010.* © 2010 Wiley-Liss, Inc.

Key words: adaptor protein complexes; AP-1; clathrin; trans-Golgi network; membrane traffic; zebrafish; gut

Accepted 10 June 2010

INTRODUCTION

In eukaryotic cells proteins are transported through secretory and endocytic pathways by transport vesicles, which bud from a donor compartment and subsequently fuse with an acceptor compartment. The formation of these transport vesicles is mediated by cytoplasmic coat proteins. Four adaptor-protein complexes have been described in higher eukaryotic organisms: AP-1, AP-2, AP-3, and AP-4 (Boehm et al., 2001; Robinson, 2004). Each complex is composed of two large chains (one each of γ/α/δ/ϵ, and β1–4, respectively, of 90 and 130 kDa), one medium-sized chain (μ1–4) of ~50 kDa and one small chain (σ1–4) of ~20 kDa, collectively referred to as "adaptins." AP-1 and AP-2 are the classical clathrin-coated-vesicle adaptor protein complexes, which recruit clathrin to the vesicle membrane. AP-2 mediates endocytosis from the plasma membrane, while AP-1, AP-3, and AP-4 mediate sorting and transport in the endosomal/lysosomal pathways (Bonifacino and Traub, 2003). In mice and humans, the ubiquitously expressed AP-1A complex is formed by γ1, β1, μ1A, and σ1A adaptins (Meyer et al. 2000; Glyvuk et al. 2010). AP-1A has been localized to the perinuclear *trans*-Golgi network (TGN) and mediates vesicular protein transport between the TGN and early endosomes. A polarized epithelia-specific complex AP-1B exists in mammals, which mediates protein exocytosis from recycling endosomes to the basolateral plasma membrane (Ohno et al., 1999; Fölsch et al., 2001; Fölsch, 2005; Deborde et al., 2008). In AP-1B, μ1A is replaced by μ1B, which is 85% identical. μ-adaptins mediate protein sorting by binding to

Additional Supporting Information may be found in the online version of this article.

[1]Department of Biomedical Sciences and Biotechnology, Unit of Biochemistry and Unit of Biology (GB), University of Brescia, Brescia, Italy
[2]Department of Biology, University of Milan, Milan, Italy
[3]Department of Biomedical Sciences and Biotechnology, Unit of Pathology, University of Brescia, Brescia, Italy
[4]Center for Biochemistry and Molecular Biology, Biochemistry II, Georg-August-University Göttingen, Göttingen, Germany

Grant sponsor: Grants 60% MIUR; Grant sponsor: "Associazione Amici per il Cuore"; Grant sponsor: C.A.R.I.P.L.O. platform Molecular Biology and Cancer Stem Cells; Grant sponsor: CARIPLO PLATFORM Molecular Biology and Cancer Stem Cells; CARIPLO Foundation (Zebragene); Grant number: DFG 802/3-1 (P.S.).

***Correspondence to: Peter Schu, Center for Biochemistry and Molecular Biology, Biochemistry II, Georg-August-University Göttingen, Göttingen, Germany. E-mail: pschu@gwdg.de or Franco Cotelli, Department of Biology, University of Milan 20133, Italy. E-mail: franco.cotelli@unimi.it**

DOI 10.1002/dvdy.22372
Published online 22 July 2010 in Wiley Online Library (wileyonlinelibrary.com).

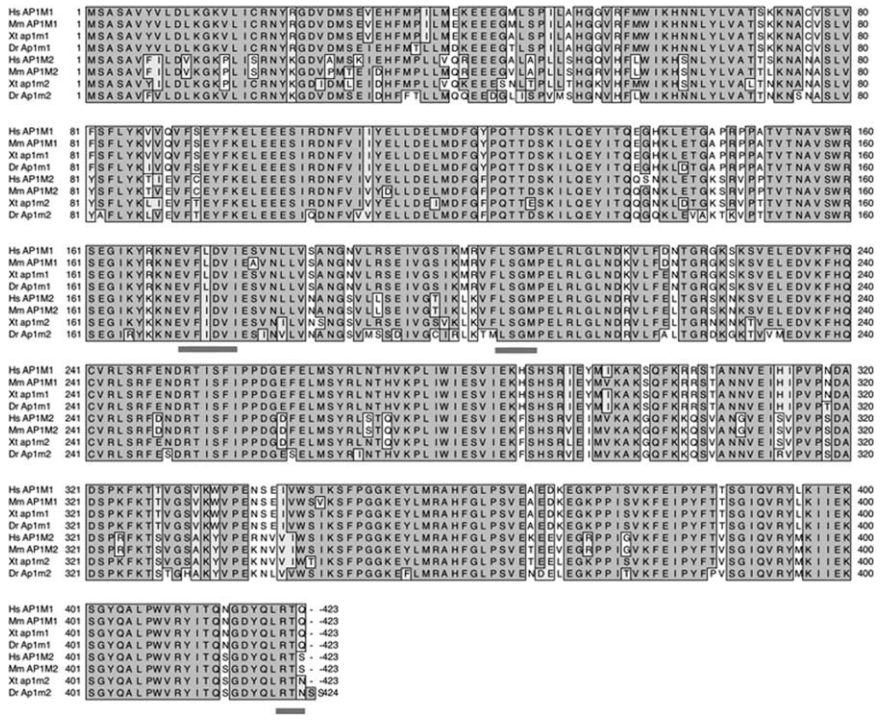

Fig. 1. Multiple alignment of vertebrate μ1 adaptins. Consensus residues were assigned based on the number of occurrences of the character in the column. Levels of shading were set to grey for 100% conservation, light grey for 80%, no shading for less than 80%. Underlined are residues essential for recognition of tyrosine-based sorting signals (see Experimental Procedures section for database entries).

tyrosine-based sorting peptide motifs. γ1 mediates AP-1 recruitement to the target membrane via binding to phosphatidylinositol 4-phosphate and the small G-protein Arf-1, which also binds to β1. Both large adaptins bind clathrin and recruit additional so-called "accessory" proteins to the site of transport vesicle formation. Besides μ1, cargo proteins are also bound by β1, γ1/ σ1 hemi-complexes and σ1 (Owen and Evans, 1998; Owen et al., 2001; Janvier et al., 2003; Doray et al., 2007; Kelly et al., 2008). AP-1A adaptin knock-out's in mice revealed that it is indispensable for mammalian development. γ1-deficient embryos cease development at day 3.5 pc, before the blastocyst hatches out of the zona pellucida. No embryonic stem cell line could be established from γ1-deficient embryos (Zizioli et al., 1999). The murine μ1A knock out is embryonic lethal during organogenesis at day 13.5 pc. This difference can be most likely attributed to the homologues μ1B-adaptin. Mouse embryonic fibroblast cell lines could be established from μ1A-deficient embryos, demonstrating that cultured murine fibroblasts do not depend on AP-1A function for viability and growth (Meyer et al., 2000). μ1B-adaptin is required for the establishment of apical-basolateral polarity in mammalian cell culture systems of kidney-derived cell lines (Fölsch, 2005). In vivo analysis of AP-1 function has also been performed in the worm *C. elegans*, which contains two μ1 genes, *unc-101* and *apm-1*. Both are close homologues, are more closely related to mammalian μ1A, than to μ1B, and are expressed ubiquitously during development. Disruption of both genes causes embryonic lethality, whereas single disruptions of either are viable. Interestingly, they have distinct phenotypes indicating that the isoforms may have distinct functions, despite their high homology (Shim et al., 2000). We decided to use zebrafish (*Danio rerio*) as an animal model to study AP-1A (μ1A) and AP-1B (μ1B) functions in low vertebrate development (Postlethwait et al., 1998). Despite their structural homologies to human and mouse μ1-adaptins, we found differing expression patterns. Zebrafish AP-1 μ1B-adaptin knock-down experiments demonstrate that μ1B-adaptin is indispensable during lower vertebrate development.

RESULTS

Identification and Characterization of Zebrafish μ1-Adaptins

The sequences of human and mouse μ1A and μ1B subunits were assembled using ENSEMBL and VEGA and then used as queries in BLAST searches at the Zebrafish Genome Browser (www.ensembl.org/Danio rerio) and in a public EST database available at the NCBI (www.ncbi.nlm.nih.gov/BLAST). The search revealed two putative sequences in zebrafish. NM-205714 encodes for a putative protein of 424 amino acids, homologous to the mammalian tissue-specific μ1B. XM-695500 encodes for a putative protein of 429 amino acids, homologous to the mammalian ubiquitously expressed μ1A. Also a search in ENSEMBL zebrafish assembly version 8 (Zv8) revealed one transcript for μ1A and one for μ1B. Both sequences share high amino acid sequence identity with human and mouse μ1 adaptins. Using in silico cloning and rapid amplification of cDNA ends (RACE) techniques, we assembled the complete coding sequences (CDS) of zebrafish μ1 adaptins. According to Zebrafish Nomenclature Guidelines (www.zebrafish.org), we designed these two genes as *ap1m1* (μ1A, XM-695500) and *ap1m2* (μ1B, NM-205714). We cloned and characterized both sequences and focused on the characterization of the tissue-specific μ1B subunit, whose function in development is not known. The deduced amino acid sequences of zebrafish μ1-adaptins were compared to vertebrate proteins from *H. sapiens, M. musculus, X. tropicalis* (Fig. 1). Multiple alignment of these sequences points out the high degree of amino acid sequence identity between zebrafish and other vertebrates. Zebrafish μ1A is 88% identical to *H. sapiens* and *M. musculus*

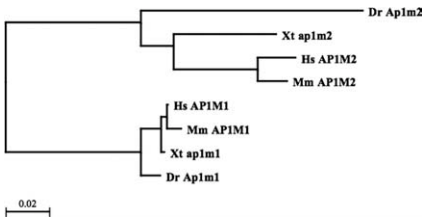

Fig. 2. Unrooted phylogenetic tree of vertebrate μ1 adaptins. The tree was generated as described in Experimental Procedures section. The horizontal bar = a distance of 0.02 substitutions per site.

orthologues, while μ1B shares an 83 and 86% identity with *H. sapiens* and *M. musculus* μ1B, respectively. AP-complexes selectively bind to the peptidic sorting signal motifs in the cytoplasmic domains of transmembrane proteins (Bonifacino and Traub, 2003). μ-adaptins bind tyrosine-based YxxØ (Ø is a large hydrophobic residue) motifs. Residues important for AP-1 functions are conserved in all species (Owen and Evans, 1998; Owen et al., 2001; Robinson, 2004). Also in zebrafish a remarkable conservation of the amino acids involved in YxxØ binding is observed. Of the 11 residues in μ1 subunits of mammals, shown to be involved in the recognition of YxxØ signals, 6 are conserved in zebrafish. These are V^{173}, F^{174},D^{176},L^{203},K^{204}, and R^{421} (Fig. 1). A phylogenetic, rooted neighbour-joining tree of the vertebrate μ1A and μ1B family of genes indicates that the *ap1m1* and *ap1m2* zebrafish genes are closely related to the human and murine genes and they probably arose by a gene duplication relatively recently, before the emergence of vertebrates (Fig. 2).

Genomic Organization

Human and murine μ1 genes exhibit a different genomic organization. The *ap1m1* and *ap1m2* human genes, which encode for μ1A and μ1B, map to the same chromosome 19 and both consist of 12 exons and 11 introns. The murine *Ap1m1* and *Ap1m2* genes are located on different chromosomes and differ in their organization. The *Ap1m2* gene consists of 11 exons and 10 introns in a region of ~21 kb. By contrast, the *Ap1m1* gene spans approximately 16 kb and consists of 12 exons and 11 introns (Nakatsu et al., 1999).

The genomic structure and the exon-intron boundaries of the zebrafish orthologues were determined by performing BlastN alignments of different of AP-1 μ1 cDNAs against the ENSEMBL zebrafish assembly version 8 (Zv8) database and then compared to the human and mouse genes. Zebrafish *ap1m1* is located on chromosome 2 while *ap1m2* is located on chromosome 6. The intron-exon structures of zebrafish genes *ap1m1* and *ap1m2* differ from mouse as *ap1m1* is organized in 11 and *ap1m2* in 12 exons.

Heterologous Expression of Zebrafish μ1B in Mammalian Cells

We tested zebrafish μ1B for adaptin function. Ectopic expression of murine μ1B is able to complement μ1A-deficiency of murine fibroblasts (μ1A −/−). In control cells AP-1A, detected by anti-γ1 antibodies, is concentrated at the perinuclear TGN (Fig. 3A). Also the mannose 6-posphate receptor MPR46, which transports lysosomal enzymes from the TGN to endosomes, is concentrated peri-nuclear at the TGN (Fig. 3B). In μ1A −/− cells, the perinuclear TGN staining of γ1 is lost and MPR46 is redistributed from the preferential perinuclear TGN localization to early endosomes. Ectopic expression of μ1A and μ1B normalizes AP-1 (γ1) and MPR46 subcellular distribution (Eskelinen et al., 2002). Zebrafish μ1B cDNA was cloned into the pcDNA3.1 expression vector and transiently expressed in μ1A-deficient mouse embryonic fibroblasts. Expression of zebrafish μ1B restored perinuclear TGN localization of AP-1 and of MPR46 (Fig. 3). These data confirm that zebrafish μ1B adaptin can perform μ1-adaptin "house-keeping" functions like the murine orthologue.

Temporal Expression Pattern of *ap1m1* and *ap1m2*

In order to analyze *ap1m1* and *ap1m2* temporal expression patterns, we performed RT-PCR assays on cDNA obtained from different developmental stages (Fig. 4A) and adult organs (Fig. 4B) using specific primers (see Experimental Procedures section). Both transcripts are detected in the embryos at the 2-cell-stage as maternal mRNA. The expression level of *ap1m1* transcript is maintained in all developmental stages examined. The *ap1m2* gene transcript level strongly decreases at the shield stage and during the somitogenesis stage, but it starts to increase at 24 hpf and is still detectable at 48 and 72 hpf. We further addressed by RT-PCR whether zebrafish *ap1m1* and *ap1m2* have different expression patterns in adult organs. As shown in Figure 4B, the RT-PCR based analysis demonstrated that only some adult organs such as the digestive system, liver, pancreas, kidney, and testis display a high content of *ap1m2* transcripts. No RT-PCR amplification was observed in brain, while in heart, eye, and skeletal muscle a very weak band is present. The *ap1m1* transcript shows a different expression pattern. It is abundant in brain, eye, skeletal muscle, testis, and heart, but no transcript is detected in liver, pancreas, and kidney. These data provide evidence that zebrafish μ1B seems to have tissue-specific functions as previously described for mouse μ1B (Ohno et al. 1999). Interestingly, also μ1A expression shows a tissue dependence in zebrafish unlike the mouse orthologue, which is ubiquitously expressed (Meyer et al. 2000).

Spatio-Temporal Expression of μ1-Adaptins During Development

To analyze the spatio-temporal expression of *ap1m1* and *ap1m2* in zebrafish tissues, whole mount in situ hybridizations were performed from the two-cell stage to 48-hpf embryos using an antisense probe. A sense probe was used in parallel control experiments, which did not produce any signal (data not shown). Starting at the 1–2-cell stage, the *ap1m1* and *ap1m2* transcripts are present until 256 cells, pointing to a maternal origin of the transcript (not shown).

Next we analyzed later stages of development at 24 and 48 hpf (Fig. 5A–E). We could observe a different staining for the *ap1m1* and *ap1m2* transcripts. At 24 hpf, *ap1m1* is mainly expressed in brain regions and the eyes (Fig. 5A). At this stage, no other structures are labelled. Labelling of *ap1m1* to the brain region becomes

more intense at 48 hpf. In accordance with RT-PCR data, a signal is now present at the gut region (Fig. 5C). At 24 hpf, expression of *ap1m2* was more intense in the restricted area of the gut and the two parallel strikes defined as pronephric ducts (Fig. 5B). At stage 24 hpf, gut endoderm coalesces at the midline, forming a tube, which loops to the left, and liver, pancreas, swim bladder, and epithelium of the gastrointestinal tract start to develop (Kimmel et al., 1995; Warga and Nüsslein-Volhard, 1999; Ober et al., 2002; Wallace and Pack, 2003). By 30 hpf, expression of *ap1m2* becomes comparable with that at the intestinal bulb and pronephric ducts (Fig. 5E) (as shown at ZFIN; Thisse et al., 2001; zgc:85644 cb782). The specific expression of *ap1m2* transcript is well maintained at 48 to 72 hpf and is still detected in the liver and the intestinal bulb (Fig. 6–D). μ1B expression in gut and pronephric ducts was to be expected, because mouse μ1B is expressed in polarized epithelial cells of fetal and adult tissues of endodermal derivation as the intestine and the kidneys. However, mouse μ1B is not expressed in fetal or adult liver (Ohno et al., 1999). Also μ1A expression in zebrafish differs from the murine expression pattern. All murine tissues express μ1A and only polarized epithelia express μ1B in addition. In conclusion, the results of whole-mount in situ hybridization and RT-PCR performed on zebrafish embryos and adult tissues provide evidence that μ1B (AP-1B) may have specific functions in endoderm-derived organs. In addition, it appears to be able to substitute for μ1A. AP-1B could be involved in sorting events necessary for the establishment and maintenance of apical-basolateral cell polarity as in mammals.

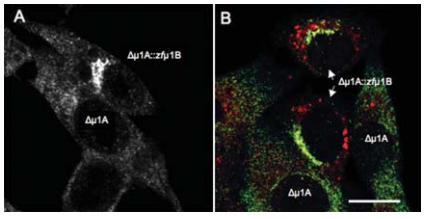

Fig. 3. Heterologous expression of *ap1m2* in mammalian cells. *ap1m2* was expressed in murine fibroblasts derived from a μ1A-adaptin knock-out mouse. In these cells, γ1-adaptin and MPR46 are not located to the peri-nuclear trans-Golgi network. **A**: Z*fap1m2* expression rescues membrane binding of γ1. **B**: Upon Z*fap1m2* expression, MPR-46 (red) is also peri-nuclear enriched (γ1 green). Scale bar = 20 μm.

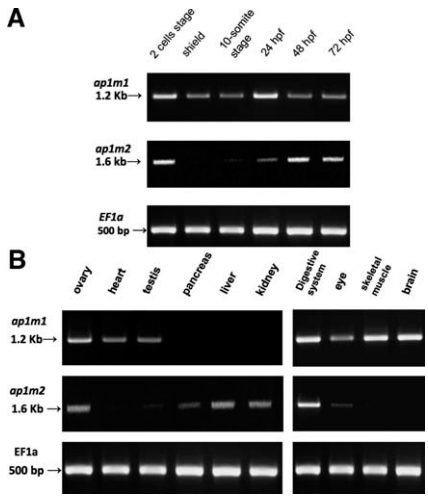

Fig. 4. *ap1m1* and *ap1m2* expression during development and in adult organs. Expression analysis by RT-PCR. α-Elongation Factor served as positive control. **A**: *ap1m1* and *ap1m2* expression during zebrafish development from 2 cells to 72 hpf. **B**: *ap1m1* and *ap1m2* expression pattern in adult organs.

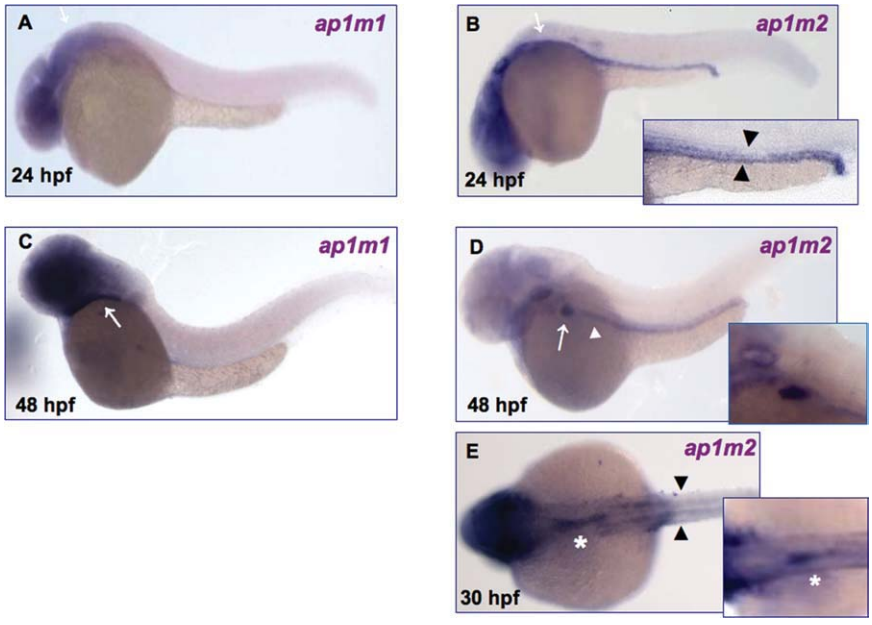

Fig. 5. Spatio-temporal expression of *ap1m1* and *ap1m2*. Whole mount in situ hybridization assays were performed on embryos at 24 and 48 hpf. **A, C**: *ap1m1* expression in brain and eye at 24 hpf (A) and 48 hpf (C). Signal is also present at 48 hpf in the gut region (white arrow). **B–E**: *ap1m2* expression. B: *ap1m2* is detected at the level of pronephric ducts (black arrowhead) and gut region (white arrow) at 24 hpf. D: White arrowhead indicates digestive tract and white arrow indicates liver at 48 hpf. E: Dorsal view. Black arrowheads indicate the pronephric ducts and white asterisk indicates the intestinal bulb at 30 hpf. All embryos (except E) are mounted lateral view anterior to the left.

ap1m2 Knock-Down Experiments

After demonstrating zebrafish *ap1m2* transcript expression in some organs of endodermal origin, we asked whether μ1B has functions during development. We employed knock-down experiments by injecting morpholino anti-sense oligonucleotides into 1–2-cell-stage embryos. An *ap1m2* morpholino sequence (*ap1m2*MO) was designed against the 5′ UTR spanning the *ap1m2* ATG start codon to inhibit protein translation. The optimum concentration was determined to 0.7 pmol/embryo. Higher *ap1m2*MO doses induced lethality. Seventy-five percent of the morpholino-injected embryos developed a consistent phenotype by 24 hpf, which persisted through 48 hpf in 87% of *ap1m2*MO embryos (Table 1). They continued to survive until 7–8 dpf. Injection of control morpholinos caused no abnormal phenotypes. *ap1m2*MO embryos show a severe reduction in mobility, leaving the *chorion* 3 to 4 hours later compared to controls. Mobility defect appears at 24 hpf and becomes more severe at 48 and 72 hpf. Phenotype is

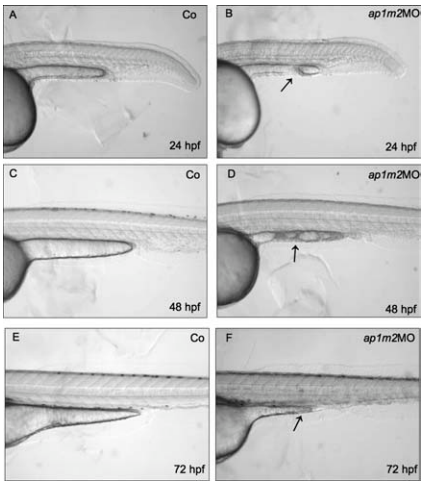

Fig. 6. *ap1m2* knock-down embryos. Morphants showed severe defects in gut tube formation and margins are not well defined. Morphants are smaller than controls. Black arrows point to particularly altered morphology. Images are at 40× magnification. Embryos are shown in lateral views, anterior to left.

TABLE 1. Summary of Phenotypes in *ap1m2* Morphant Embryos (Translation-Blocking Morpholino)[a]

Control	*ap1m2*MO	24 hpf	*ap1m2*MO 48 hpf
Injected embryos	110	115	115
Morphological defects	3 (2%)	75 (65%)	87 (76%)
Reduced mobility	0	65 (57%)	75 (65%)

[a]One- to two-cell-stage zebrafish embryos were injected with 0.7 pmol/embryo of *ap1m2*MO. Data are expressed as percentage of morphants showing the indicated defects of gut and organs of endodermal derivation at the respective hpf. Data are from five independent experiments.

TABLE 2. Summary of Phenotypes in *ap1m2* Morphant Embryos (Splicing-Inhibiting Morpholino)[a]

Control	*ap1m2*MOs	24 hpf	*ap1m2*MOs 48 hpf
Injected embryos	125	120	120
Morphological defects	4 (3.2 %)	90 (75%)	95 (79%)
Reduced mobility	0	80 (67%)	75 (62,5%)

[a]One- to two-cell-stage zebrafish embryos were injected with 0.5 pmol/embryo of *ap1m2*MOs (splicing-inhibiting morpholino). Data are expressed as percentage of morphants showing the indicated defects of digestive tract and organs of endodermal derivation at the respective hpf. Data are from six independent experiments.

maintained until 7–8 dpf and embryos cease development. The gut tube appears to be abnormal at 24 hpf and by 48–72 hpf its formation is still not completed. It is smaller and margins are not defined (Fig. 6A–F). In contrast, many other tissues appear to be normal. These include notochord, neural tube, body wall muscle, and the nervous system. Later in development, mutants exhibit widespread defects in morphogenesis and differentiation of the liver and the pancreas, indicating that *ap1m2* is required for proper maturation of these organs. By 2–3 dpf, every injected embryo is distinguished by a kinky tail and development is delayed, leading to embryos that are ~25% smaller than controls. To support the specificity of the phenotype, we performed whole-mount in situ hybridization using two different probes: *pax2a* and *prox1*. Zebrafish *pax2a* (*paired box gene 2a*) is a good marker for pronephric ducts (as shown by Mujumdar et al., 2000; ZFIN cb 378) (Stickney et al., 2007). As shown in Figure 7, *ap1m2* morphants show a severely reduced staining of pronhephric ducts. Also labelling of the abnormal gut with *pax2a* is strongly reduced in morphants with respect to controls. Zebrafish *prox1* is a transcription factor, which exerts a role in the differentiation of a variety of embryonic tissues such as central nervous system, sensory organs, and tissue of non-neuroectodermal-origin, like liver, pancreas, gut and gills (Pistocchi et al., 2008). As shown in Figure 8, the *ap1m2*MO morphants show a severe reduction in staining of the liver and pancreas compared to controls at 48 hpf. These results demonstrate a role of μ1B in zebrafish development during the formation of organs such as liver, pancreas, gut, and pronephric ducts. We also analysed *ap1m1* transcript levels in *ap1m2* morphants at 24 and 48 hpf. Staining of *ap1m1* in *ap1m2* morphants is the same as in controls (Fig. 9), demonstrating that expression of the two adaptins in zebrafish is controlled independent of each other and indicating that they have specific functions in the respective tissues.

In order to confirm these results obtained with translation blocking morpholino, we also used splice-inhibiting morpholino. The optimum dose to be injected was determined to 0.5 pmol/embryo. As shown in Figure 10, we could demonstrate by RT-PCR the splice-blocking activity of the *ap1m2*-MOs. These morphants show the same severe phenotypes as the morphants of translation-blocking morpholino. The percentage of *ap1m2*MOs showing defects is very similar to the percentage of *ap1m2*MO morphants (Table 2). The phenotype in the gut region is reproduced and development is severely compromised at 24 and 48 hpf: the gut region appears smaller and abnormal in size and the yolk appears to be reduced in size and sometimes collapsed (see Supp. Fig. S1A–D, which is available online). Histological sections of the gut region in *ap1m2*MOs (Fig. S2) also demonstrate a smaller and less-organized tissue as well as a collapsed pronephric duct. The poor development of these tissues is reminiscent of the failure of μ1B-deficient mammalian kidney cell lines to form a polarized, apical-basolateral cell monolayer in cell culture (Fölsch, 2005).

DISCUSSION

In eukaryotic cells, intracellular membrane traffic is mediated by transport vesicles and the formation of transport vesicles requires multicomponent adaptor-protein complexes (AP-1, AP-2, AP-3, AP-4). The AP-1 is responsible for transport between the

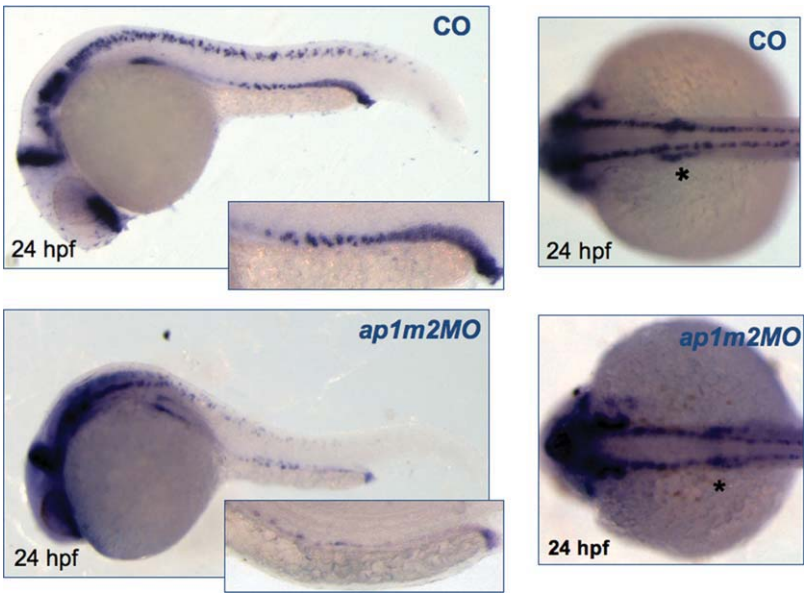

Fig. 7. *pax2a* staining in control and *ap1m2*MO embryos. Expression of *pax2a* in morphants is severley reduced compared to controls at 24 hpf especially in the region of pronephric ducts (*). Embryos are shown anterior to the left and dorsal up.

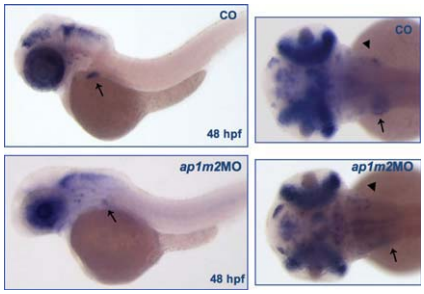

Fig. 8. *prox1* staining in control and *ap1m2*MO embryos. The expression of *prox1* in morphants is reduced compared to controls at 48 hpf in liver (black arrows) and pancreas (black arrowheads). Embryos are shown anterior to the left and dorsal up at 25× fold magnification.

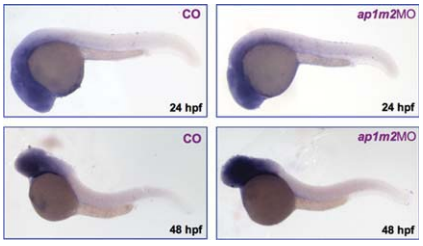

Fig. 9. Expression level of *ap1m1* transcript in *ap1m2* morphants. *ap1m1* expression at 24 and 48 hpf and in *ap1m2* morphants. Embryos are shown anterior to the left.

TGN and early endosomes. μ1A knock-out mice cease development in utero at day 13.5 pc. All organanlagen are present, but embryos are smaller than their wild-type litter-mates and show hemorrhages in the ventricles and the spinal canal. Fibroblast cell lines could be established from these embryos. The remaining three AP-1 adaptins are not functional as indicated by the absence of γ1-adaptin subunit membrane binding and by severe missorting of mannose 6-phosphate receptors MPR46 and MPR300. Due to a block in retrograde early endosome to TGN transport, both are redistributed into an endosome plasma membrane recycling pool, dramatically enhancing MPR300 endocytic capacity (Meyer et al., 2000, 2001). This may contribute to phenotype development, because the essential function of MPR300 is mediating the endocytosis and subsequent degradation of excess IGF-II. In addition, it binds LIF, retinoic acid, and most of its 15 ligand-binding cassettes are still orphans (Ghosh et al., 2003). μ1B expression is restricted to polarized epithelial cells. In kidney-derived cell lines, it mediates basolateral exocytosis of proteins from recycling endosomes. It is essential for the establishment and maintenance of apical-basolateral polarity and, e.g., mediates the basolateral sorting and transport of tight-junction proteins and the low-density-lipoprotein receptor (Fölsch, 2005). However, μ1B can also perform house-keeping functions in fibroblasts normally performed by μ1A (Eskelinen et al., 2002; Fig. 3). μ1B function in mammalian development has not been tested yet.

We report the characterization and functional analysis of zebrafish μ1B (*ap1m2* gene). In silico analysis revealed two genes, which encode for two proteins with high identity to mammalian μ1-adaptins, the ubiquitously expressed μ1A and the polarized epithelia-specific isoform μ1B. Gene organization in zebrafish is similar to the genomic organization in human and mouse. Zebrafish μ1A and μ1B expression analysis revealed tissue-dependent expression patterns for each of them. *ap1m1* and *ap1m2* transcripts are expressed from early stages (1–2 cells) until later stages of development (48–72 hpf), but in adult tissues only one of them is expressed at detectable levels. The *ap1m1* transcript is present in brain regions and the eye. No *ap1m1* staining is present in liver or pronephric ducts. *ap1m2* staining is restricted to the midline at 24 hpf, where organs of endodermal origin such as gut, pharyngeal endoderm, and pronephric duct will develop (Tam et al., 2003). Zebrafish *ap1m2* morphants show a severe phenotype. Development is delayed and embryos are approximately 25% smaller than controls. At 24 and 48–72 hpf, *ap1m2MO* morphants exhibit widespread defects in morphogenesis and differentation of endoderm-derived organs. From 24 hpf on, they show reduced mobility, which became more severe during later stages and embryos die at 7–8 dpf.

Zebrafish μ1A and μ1B adaptins are structurally highly homologous to their mammalian orthologues, yet their expression patterns differ in two ways. Firstly, all murine tissues express μ1A and polarized epithelia express in addition to μ1A also μ1B (Ohno et al., 1999, Meyer et al., 2000). Thus, zebrafish μ1A function is either not required in those tissues expressing only μ1B, or μ1B is able to fullfill μ1A functions as well. The latter interpretation is more likely as murine and zebrafish μ1B adaptins are able to substitute at least for μ1A house-keeping functions in fibroblasts (Eskelinen et al. 2002; Fig. 3). Secondly and surprisingly, μ1B is expressed in zebrafish liver, whereas mouse μ1B is not expressed in fetal or

adult liver. μ1B expression in organs such as intestine and pronephric duct was to be expected, because of the murine expression pattern (Ohno et al., 1999). It is intriguing to speculate that during evolution of lower vertebrate to higher vertebrate, μ1B expression was lost in polarized cells of fetal and adult liver and that new, μ1B-independent mechanisms developed to ensure basolateral sorting in the developing liver and differentiated hepatocytes. One major difference in establishing cell polarity between mammalian hepatocytes and mammalian epithelial cells, e.g., kidney and gut, is the sorting organelle. In polarized epithelial cells apical-basolateral sorting decisions are made already at the trans-Golgi network, whereas hepatocytes transport all proteins from the trans-Golgi network first to the basolateral domain, then they are endocytosed, and apical-basolateral sorting decisions are made in basolateral and apical endosomes (Fölsch, 2005; Mellman and Nelson, 2008; Deborde et al., 2008). Zebrafish hepatocytes appear to sort and transport proteins by mechanisms similar to those in polarized epithelial cells. Comparing mammalian and zebrafish AP-1 functions should reveal insights into the development of polarized sorting mechanisms and vertebrate evolution.

EXPERIMENTAL PROCEDURES

Zebrafish Embryo Maintenance and Collection

Zebrafish were raised and maintained under standard laboratory conditions at 28°C (Westerfield, 1995) and bred by natural crosses. Immediately after spawning, fertilized eggs were harvested, washed, and placed in 10-cm Ø Petri dishes in fish water. Developing embryos were incubated at 28°C. Collected embryos were stored in 0.003% phenyl-thiourea (PTU) (Sigma, St. Louis, MO). Solution blocks pigment formation, which improves visualization of RNA in whole-mount in situ hybridization. The embryo stages were identified by morphological features and the corresponding embryos were fixed in 4% paraformaldehyde (PFA/PBS) overnight at 4°C, rinsed twice in PBS + 1% Tween-20 (PBT), then dehydrated in methanol and stored at −20°C until processing.

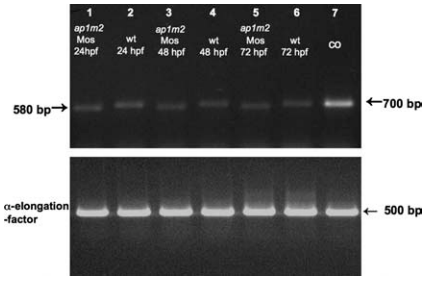

Fig. 10. *ap1m2* expression in wild type and morphants embryos. Splice-inhibiting morpholino was designed to exclude exon 3. cDNA was prepared from 24-, 48-, and 72-hpf injected-embryos and controls (see Experimental Procedures section). The expected bands were 700 bp for wild type embryos and 580 bp for injected embryos. α-Elongation-factor 1a (EF1a) serves as control.

Cloning and Sequencing of Zebrafish *ap1m1* and *ap1m2* Genes

Total RNA was isolated from pooled embryos and adult organs using Trizol® Reagent (Invitrogen, Carlsbad, CA). For 5′ RACE technique FirstChoice RLMRACE kit was used (Ambion, Austin, TX). Reverse transcriptase reaction was performed with 1 μg total mRNA for 45 sec at 37°C in a final volume of 25 μl in the presence of random hexamer oligonucleotides. PCR amplification of full-length cDNA's: *ap1m1* primers were $AP1M1L_4$ 5′-CTGCCGTAATAACCGC GGGGATGTGGAC-3′ and $AP1M1\text{-}R_7$ 5′-CCATGAATGCGAGCTGTAGCC-3′; 30 sec at 94°C, 30 sec at 60°, 90 sec at 72°C, 35 cycles. *ap1m2* primers were $APG7L_3$ 5′-GGAATGTGACTTTAA-CTCTGCTT TAGCC-3′ and $APG7R_4$ 5′-CGATTTA TTACAGCATTAGGA-GAAACAG-3′; 30″ at 94°C, 30″ at 60°C, and 90″ at 72°C, 35 cycles. PCR products were cloned directly into pGEM®-T Easy vector (Promega, Madaison, WI) and sequenced using Big Dye terminator v3.1 protocol on ABI PRISM 310 Genetic Analyzer (Applied Biosystems, Foster City, CA).

Bioinformatic Analysis of Zebrafish *ap1m1* and *ap1m2*

Nucleotide and amino acid sequences were compared to the non-redundant sequence databases present at the NCBI (National Center for Biotechnology Information. GenBank database) using BLAST version 2.0 (Altschul et al., 1990) and ENSEMBL zebrafish assembly version 8 (Zv8). Sequences annotated as putative *ap1m1* and *ap1m2* genes were extracted and enriched with sequences coming from Ensembl Database of genome projects (http://www.ensembl.org). The multiple sequence alignment was performed using CLUSTALW algorithm (Thompson et al., 1994). Briefly, the multiple sequence alignment was generated using generated using MUSCLE (version 3.6) (Edgar, 2004), alignment refinement was obtained using Gblocks (Castresana, 2000), and phylogenetic reconstruction was performed using the maximum likelihood program PhyML (Guindon and Gascuel, 2003). The final version of the alignment was prepared using Espript (Gouet et al., 2003; Edgar, 2004). Zebrafish *ap1m1* (Acc. No. XP_700592) was compared to those of human (Acc. No. NP_115882.1), mouse (Acc. No. NP_031482), and *Xenopus tropicalis* (Acc. No. NP_989033), and zebrafish *ap1m2* (Acc No. NP_991277) was compared to those of human (Acc. No. NP_005489.2), mouse (Acc.No. NP_003808), and *Xenopus tropicalis* (Acc.No. NP_001006851.1). The phylogenetic tree was generated using MEGA 4.1 program with Neighbor-Joining (NJ) method.

Multi-tissue RT-PCR

PCR was performed on cDNAs (see above): *ap1m1* primers: AP1M1-F7 5-′GTCCGTTAACCTCCTGGTCAGTG-3′, AP1M1-R7 5′-CCATGAATGCGAG CTGTAGCC -3′. *ap1m2* primers: AP1G7L4 5′-CGGTGTTCGTGCTGG ACCTGAAGGGG- 3′, AP1G7R4 5′-CGATTTATTACAGCATTAGGAGAA ACAG-3′. α-*Elongation Factor 1a* (*EF1*α) was used as positive control, using specific primers as described (Gilardelli et al., 2004).

Construct, Transfection, and Microscopy

Zebrafish *ap1m2 pcDNA* expression vector was constructed by subcloning full-length cDNA in pGEM®-T Easy vector and an excised *Eco*RI fragment was cloned in pcDNA 3.1 expression vector. *ap1m2 pcDNA* was verified by

sequencing both strands using Big Dye terminator v3.1 protocol on ABI PRISM 310 Genetic Analyzer (Applied Biosystems).

ap1m2 pcDNA3.1 was transfected into μ1A−/− mouse embryonic fibroblasts by the Effectene Tranfection Kit (Quiagen, Chatsworth, CA) (Meyer et al., 2000). For microscopic analysis, cells were fixed with *p*-formaldehyde and permeabilized with saponin following standard protocols. Adaptins were detected with anti γ-1 mouse monoclonal antibodies (BD Transduction Laboratories, San Diego, CA). Anti-MPR46 were generously provided by R. Pohlmann. Fluorophore-coupled secondary antibodies were from Jackson Immunoresearch. Confocal microscopy was performed using a Leica *DRM IRE2* TCS SP2 with a Plan Apochromat 63×/1.40 (Leica, Bensheim, Germany).

Whole-Mount In Situ Hybridization

Single hybridizations and detections were carried out on wild-type embryos. Antisense and sense riboprobes were prepared by in vitro transcribing linearized cDNA clones with T7 and SP6 polymerase using Digoxigenin Labelling Mix (Roche). *ap1m1* anti-sense probe: 824-bp fragment amplified with AP1F7 5′ GTCCGTTA ACCTCCTGGTCAGTG and AP1R7 5′ CCATGAATGCGAGCTGTAGCC 3′ and subcloned in pGEM®-TEasy vector. Probe was synthesized with T7 Polymerase by transcribing the *Not* I linearized pGEM®-TEasy *ap1m1*. *ap1m2* anti-sense probe containing the ATG was synthesized with T7 polymerase by transcribing the SacI-linearized pGEM®-TEasy *ap1m2*. The corresponding sense probe was synthesized with SP6 RNA polymerase using a *Apa* I linearized pGEM®-TEasy *ap1m2*. *ap1m2*RNA probe: 702-bp fragment, amplified by PCR with primers AP47L 5′-CCGCTAAA-CACCGGAATGTGACTTTAC-3′ and AP47R 5′-GGGCTGTCGTAGCAGA AGTCAGACTAC-3′. Whole-mount *in situ* hybridization was carried out as previously described (Thisse et al., 1993). In brief, embryos were treated with 0.003% phenylthiourea (PTU) to prevent pigmentation. After fixation, embryos older than 24 hr were permeabilized with Proteinase K (10 μg/ml, Sigma) and hybridized overnight at 68°C in formamide buffer with Digoxigenin-Labeled RNA antisense or sense probes. After several washes at high stringent temperature, NBT/BCIP (Roche, Nutley, NJ) staining was performed according to the manufacturer's instructions. Embryos were mounted in agarose-coated dishes and photographated under Leica MZ16 F stereomicroscope (1 × Plan Apo objective, NA 0.141) equipped with DFC480 digital camera and ICM50 software version 2.8.1. (Leica, Wetzlar, Germany). *prox1*-sense 5′-ACCTCAGCCACCATCGTT CCATC-3′ and *prox1*-antisense 5′-CA CTATTCATGCAGAAG-CTCCTGC-3′. PCR products was sucloned in pGEM®-TEasy and used for labelling probe (Roche) (Pistocchi et al., 2008).

Morpholino Design and Microinjections

Antisense morpholino (MO) oligonucleotides (Gene Tools, Corvallis, OR) were directed against the 5′-untraslated region (UTR) spanning the *ap1m2* ATG start codon (5′-CGCGGACGCA GACATACTGTACTG TACGCT-3′). MOs, diluted in Danieau buffer, were injected at the 1- to 2-cell stage. Escalating doses of each MO were tested for phenotypic effects (0.5 pmol/embryo, 0.7 pmol/embryo, 1 pmol/embryo, and 1.5 pmol/embryo). *ap1m2*MO was microinjected in 4 nL volume into 1- to 2-cell-stage embryos at the concentration of 0.7 pmol/embryo. This concentration was used in all experiments because survival of the embryos was satisfactory (>86 %). Each experiment was performed in parallel with a std-MO (standard control oligo) (Gene Tools, Corvallis, OR) (5′–CCTCTTACCTCAGTTACAATTTA TA-3′) with no target in zebrafish embryos.

A splicing-inhibiting morfolino (*ap1m2*MOs) was designed to exclude exon 3 from the mature RNA, in this case a truncated protein would be formed before a stop codon is encountered.. The exon/intron sequence of *ap1m2* is available at Ensembl assembly zebrafish version 8 (Zv8): (ENSDART00000097470). In morphants, embryos deletion of exon 3 has been checked by PCR using two specific primers R2Mos*ap1m2* (5′-CGACGGA CAGCAAGATCCTGCAGG-3′) and F1Mos*ap1m2* (5′-CACAGTCGTGTG GAGATCATGG-3′) designed, respectively, upstream and downstream exon 3. The expected PCR bands were 700 bp for wild type exon 3 and 580 bp for skipped exon 3 (Fig. 9). The cDNA was prepared from 24-, 48-, and 72-hpf-injected embryos and control embryos. Escalating doses of *ap1m2*-MOs (splicing-inhibiting morfolino) were tested for phenotypic effects (0.5 pmol/embryo, 0.7 pmol/embryo, 1 pmol/embryo, and 1.5 pmol/embryo). *ap1m2*MOs was microinjected in 4 nL volume into 1- to 2-cell-stage embryos at a concentration of 0.5 pmol/embryo.

ACKNOWLEDGMENTS

We like to thank Dott.ssa Anna Pistocchi (University of Mailand) for prox1 probe.

REFERENCES

Altschul SF, Gish W, Miller W, Myers EW, Lipman DJ. 1990. Basic local alignment search tool. J Mol Biol 215:403–410.

Boehm M, Aguilar RC, Bonifacino JS. 2001. Functional and physical interactions of the adaptor protein complex AP-4 with ADP-ribosylation factors (ARFs). Embo J 20:6265–6276.

Bonifacino JS, Traub LM. 2003. Signals for Sorting of Transmembrane Proteins to Endosomes and Lysosomes. Annu Rev Biochem 72:395–447.

Castresana J. 2000. Selection of conserved blocks from multiple alignments for their use in phylogenetic analysis. Mol Biol Evol 17:540–552.

Deborde S, Perret E, Gravotta D, Deora A, Salvarezza S, Schreiner R, Rodriguez-Boulan E. 2008. Clathrin is a key regulator of basolateral polarity. Nature 452:719–725

Doray B, Lee I, Knisely J, Bu G, Kornfeld S. 2007. The γ/δ1 and α/σ2 hemicomplexes of clathrin adaptors AP-1 and AP-2 harbor the dileucine recognition site. Mol Biol Cell 18:1887–1896.

Edgar RC. 2004. MUSCLE: multiple sequence alignment with high accuracy and high throughput. Nucleic Acids Res 32:1792–1797.

Eskelinen EL, Meyer C, Ohno H, von Figura K, Schu P. 2002. The polarized epithelia-specific μ1B-adaptin complements μ1A-deficiency in fibroblasts. EMBO Rep 3:471–477.

Fölsch H. 2005. The building blocks for basolateral vesicles in polarized epithelial cells. Trends Cell Biol 15:222–228.

Fölsch H, Pypaert M, Schu P, Mellman I. 2001. Distribution and function of AP-1 clathrin adaptor complexes in polarized epithelial cells. J Cell Biol 152:595–606.

Ghosh P, Dahms NM, Kornfeld S. 2003. Mannose 6-phosphate receptors: new twists in the tale. Nat Rev Mol Cell Biol. 4:202–212.

Gilardelli CN, Pozzoli O, Sordino P, Matassi G, Cotelli F. 2004. Functional and hierarchical interactions among zebrafish vox/vent homeobox genes. Dev Dyn 230:494–508.

Glyvuk N, Tsytsyura, Y, Geumann C, D'Hooge R, Hüve J, Kratzke M, Baltes J, Boening D, Klingauf, J, Schu P. 2010. AP-1/σ1B Adaptin mediates endosomal Synaptic Vesicle Recycling, Learning and Memory. EMBO J. 29: 1318–1330

Gouet P, Robert X, Courcelle E. 2003. ESPript/ENDscript: Extracting and rendering sequence and 3D information from atomic structures of proteins. Nucleic Acids Res 31:3320–3323.

Guindon S, Gascuel O. 2003. A simple, fast, and accurate algorithm to estimate large phylogenies by maximum likelihood. Syst Biol 52:696–704.

Janvier K, Kato Y, Boehm M, Rose JR, Martina JA, Kim BY, Venkatesan S, Bonifacino JS. 2003. Recognition of dileucine-based sorting signals from HIV-1 Nef and LIMP-II by the AP-1 γ-σ1 and AP-3 δ-σ3 hemicomplexes. J Cell Biol 163:1281–1290.

Kelly BT, McCoy AJ, Späte K, Miller SE, Evans PR, Höning S, Owen DJ. 2008. A structural explanation for the binding of endocytic dileucine motifs by the AP2 complex. Nature 456: 976–979.

Kimmel CB, Ballard WW, Kimmel SR, Ullmann B, Schilling TF. 1995. Stages of embryonic development of the zebrafish. Dev Dyn 203:253–310.

Majumdar A, Lun K, Brand M, Drummond IA. 2000. Zebrafish no isthmus reveals a role for pax2.1 in tubule differentiation and patterning events in the pronephric primordia. Development 127:2089–2098.

Mellman I, Nelson WJ. 2008 Coordinated protein sorting, targeting and distribution in polarized cells. Nat Rev Mol Cell Biol 9:833–845

Meyer C, Zizioli D, Lausmann S, Eskelinen EL, Hamann J, Saftig P, von Figura K, Schu P. 2000. μ1A adaptin-deficient mice: lethality, loss of AP-1 binding and rerouting of mannose 6-phosphate receptors. EMBO J 19:2193–2203.

Meyer C, Eskelinen EL, Guruprasad MR, von Figura K, Schu P. 2001. μ1A deficiency induces a profound increase in MPR300/IGF-II receptor internalization rate. J Cell Sci 114:4469–4476.

Nakatsu F, Kadohira T, Gilbert DJ, Jenkins NA, Kakuta H, Copeland NG, Saito T, Ohno H. 1999. Genomic structure and chromosome mapping of the genes encoding clathrin-associated adaptor medium chains mu1A (Ap1m1) and mu1B (Ap1m2). Cytogenet Cell Genet 87:53–58.

Ober EA, Field HA, Stainier DY. 2003. From endoderm formation to liver and pancreas development in zebrafish. Mech Dev 120:5–18.

Ohno H, Tomemori T, Nakatsu F, Okazaki Y, Aguilar RC, Fölsch H, Mellman I, Saito T, Shirasawa T, Bonifacino JS. 1999. μ1B, a novel adaptor medium chain expressed in polarized epithelial cells. FEBS Lett 449:215–220.

Owen DJ, Evans PR. 1998. A structural explanation for the recognition of tyrosine-based endocytotic signals. Science 282:1327–1332.

Owen DJ, Setiadi H, Evans PR, McEver RP, Green SA. 2001. A third specificity-determining site in μ2 adaptin for sequences upstream of YxxQ sorting motifs. Traffic 2:105–110.

Pistocchi A, Gaudenzi G, Carra S, Bresciani E, Del Giacco L, Cotelli F. 2008. Crucial role of zebrafish prox1 in hypothalamic catecholaminergic neurons development. BMC Dev Biol 8:27.

Postlethwait JH, Yan YL, Gates MA, Horne S, Amores A, Brownlie A, Donovan A, Egan ES, Force A, Gong Z, Goutel C, Fritz A, Kelsh R, Knapik E, Liao E, Paw B, Ransom D, Singer A, Thomson M, Abduljabbar TS, Yelick P, Beier D, Joly JS, Larhammar D, Rosa F, Westerfield M, Zon LI, Johnson SL, Talbot WS. 1998. Vertebrate genome evolution and the zebrafish gene map. Nat Genet 18:345–349.

Robinson MS. 2004. Adaptable adaptors for coated vesicles. Trends Cell Biol 14: 167–174.

Shim J, Sternberg PW, Lee J. 2000. Distinct and redundant functions of mu1 medium chains of the AP-1 clathrin-associated protein complex in the nematode *Caenorhabditis elegans*. Mol Biol Cell 11:2743–2756.

Stickney HL, Imai Y, Draper B, Moens C, Talbot WS. 2007. Zebrafish bmp4 functions during late gastrulation to specify ventroposterior cell fates. Dev Biol 310: 71–84.

Tam PP, Kanai-Azuma M, Kanai Y. 2003. Early endoderm development in vertebrates: lineage differentiation and morphogenetic function. Curr Opin Genet Dev 13:393–400.

Thisse C, Thisse B, Schilling TF, Postlethwait JH. 1993. Structure of the zebrafish snail1 gene and its expression in wild-type, spadetail and no tail mutant embryos. Development 119: 1203–1215.

Thompson JD, Higgins DG, Gibson TJ. 1994. CLUSTAL W: improving the sensitivity of progressive multiple sequence alignment through sequence weighting, position-specific gap penalties and weight matrix choice. Nucleic Acids Res 22:4673–4680.

Wallace KN, Pack M. 2003. Unique and conserved aspects of gut development in zebrafish. Dev Biol 255:12–29.

Warga RM, Nüsslein-Volhard C. 1999. Origin and development of the zebrafish endoderm. Development 126:827–838.

Westerfield M. 1995. The zebrafish book. Portland: University of Oregon Press.

Zizioli D, Meyer C, Guhde G, Saftig P, von Figura K, Schu P. 1999. Early embryonic death of mice deficient in γ-adaptin. J Biol Chem 274:5385–5390.